Ecotoxicology and Environmental Safety 207 (2021) 111301

Contents lists available at ScienceDirect

Ecotoxicology and Environmental Safety

journal homepage: www.elsevier.com/locate/ecoenv

Effect of cadmium in the microalga *Chlorella sorokiniana*: A proteomic study

Antonio León-Vaz [a], Luis C. Romero [b], Cecilia Gotor [b], Rosa León [a], Javier Vigara [a,*]

[a] Laboratory of Biochemistry, Faculty of Experimental Sciences, Marine International Campus of Excellence and REMSMA, University of Huelva, 210071, Huelva, Spain
[b] Instituto de Bioquímica Vegetal y Fotosíntesis, Consejo Superior de Investigaciones Científicas and Universidad de Sevilla, Avenida Américo Vespucio, 49. 41092, Seville. Spain

ARTICLE INFO

Keywords:
Microalgae
Chlorella sorokiniana
Heavy metal
Cadmium
Proteomics
Oxidative stress

ABSTRACT

Cadmium is one of the most common heavy metals in contaminated aquatic environments and one of the most toxic contaminants for phytoplankton. Nevertheless, there are not enough studies focused on the effect of this metal in algae. Through a proteomic approach, this work shows how Cd can alter the growth, cell morphology and metabolism of the microalga *Chlorella sorokiniana*. Using the sequential window acquisition of all theoretical fragment ion spectra mass spectrometry (SWATH-MS), we concluded that exposure of *Chlorella sorokiniana* to 250 μM Cd^{2+} for 40 h caused downregulation of different metabolic pathways, such as photosynthesis, oxidative phosphorylation, glycolysis, TCA cycle and ribosomal proteins biosynthesis. However, photorespiration, antioxidant enzymes, gluconeogenesis, starch catabolism, and biosynthesis of glutamate, cysteine, glycine and serine were upregulated, under the same conditions. Finally, exposure to Cd also led to changes in the metabolism of carotenoids and lipids. In addition, the high tolerance of *Chlorella sorokiniana* to Cd points to this microalga as a potential microorganism to be used in bioremediation processes.

1. Introduction

Heavy metals are one of the most toxic contaminants due to their persistence and harmful effects on human health and the environment, especially aquatic ecosystems. Increasing industrialization and anthropogenic activities are causing alterations in biogeochemical cycles, producing high amounts of heavy metals and high levels of pollution in soils and water (Alqadami et al., 2018). Heavy metal contamination comes mainly from industrial effluents, such as metallurgical or mining wastes, as well as from urban wastewaters (Ali et al., 2013). Different studies have focused on the removal of these compounds by chemical precipitation, membrane filtration, biotransformation or bioadsorption (Gao et al., 2018; Olguín and Sánchez-Galván, 2012; Ye et al., 2017). On the other hand, plants and microorganisms, including microalgae, have been used for the bioremediation of heavy metals, with varying degrees of success (Li et al., 2020).

One of the most toxic heavy metals is cadmium, which has been shown to be a carcinogenic, mutagenic and endocrine-disrupting element (Tchounwou et al., 2012). Furthermore, Cd can cause lung damage, fragile bones or affect the regulation of calcium in biological systems (Dixit et al., 2015). In addition, it has been reported that Cd can be toxic to plants and microorganisms, reducing the photosynthetic activity and growth rate, causing oxidative stress and DNA damage, and interfering with cellular metabolism (Gutsch et al., 2018; Marchello et al., 2018). Furthermore, the accumulation of Cd in microalgae and other microorganisms, which are at the first steps of the trophic chain, can have a major impact on the ecosystems (Newton and McClary, 2019).

Chlorella sorokiniana (*C. sorokiniana*) is a robust microalga with the capacity to grow in a broad range of temperatures and environmental conditions, including industrial or urban wastewater (Izadpanah et al., 2018; León-Vaz et al., 2019). Moreover, it has been reported that this microalga can tolerate high amounts of different heavy metals, such as Zn^{+2}, Cu^{+2}, Ni^{+2} or Cr^{+3} (Akhtar, 2004; Akhtar et al., 2008; Yoshida et al., 2006). In addition, physiological studies have shown that, in the presence of Cd, photosynthesis is inhibited and the respiration rate and synthesis of cysteine or glutamate are upregulated (Carfagna et al., 2013). Nevertheless, there has been no full proteomic study about the different metabolic pathways when this microalga is cultivated with Cd. In this context, proteomics has emerged as a powerful tool for a better understanding of the metabolic responses, tolerance and detoxification mechanisms in microalgae under metal stress. Label-free proteomics, based on liquid chromatography and mass spectrometry analysis, presents a wide range of advantages compared to 2D-electrophoretic

* Corresponding author.
E-mail addresses: vigara@uhu.es, vigara65@gmail.com, vigara@uhu.es, vigara65@gmail.com (J. Vigara).

https://doi.org/10.1016/j.ecoenv.2020.111301
Received 11 May 2020; Received in revised form 3 September 2020; Accepted 5 September 2020
Available online 17 September 2020

studies: a higher number of proteins can be simultaneously studied without the gel-to-gel variations of the electrophoretic technique, and it improves the quantitative analysis (Ahsan et al., 2009; Li et al., 2018; Wase et al., 2014). This technique has been widely used to compare the expression of proteins under different environmental stimuli, and their effects on different metabolic pathways in microorganisms or plants (Aroca et al., 2017; Singh et al., 2016). Furthermore, it has been previously shown that the sequential window acquisition of all theoretical fragment ion spectra mass spectrometry (SWATH-MS) provides a more reproducible coverage of proteins than data-dependent analysis (DDA) MS (Krasny et al., 2018). To date, few studies have focused on microalgae (Anand et al., 2017; Poirier et al., 2018). For that reason, in the present study, the full proteome of *C. sorokiniana* was obtained when the microalga was cultivated in the presence of 250 μM Cd and compared with the proteome of the microalga grown in standard conditions using the SWATH-MS technique. The differences observed will help to understand the responses of *C. sorokiniana* to Cd exposure. The pathways that exhibited major differences are photosynthesis, photorespiration, oxidative phosphorylation, antioxidant system, C, N and S assimilation, amino acid biosynthesis, lipid and carotenoid metabolism and the stability of ribosomes.

2. Materials and methods

2.1. Algal strain and standard culture conditions

The *C. sorokiniana* 211-32 strain was obtained from the culture collection of the Institute of Plant Biochemistry and Photosynthesis (IBVF; Seville, Spain) and grown mixotrophically in liquid Tris-acetate-phosphate (TAP) medium (Harris, 2009), optimized for this microalga (León-Vaz et al., 2019). The microalgae were cultured at 27 °C under agitation at 150 rpm and continuous white light irradiation at 150 μE m^{-2} s^{-1}. Light intensity was measured by a Delta OHM quantum photo radiometer HD 9021, equipped with an LP 9021 PAR sensor (Delta OHM, Italy). Pre-inocula were incubated for 3 d before the experiments and inoculated into the medium to obtain an initial concentration of 1.2 ± 0.2 g L^{-1} dry weight (DW). The addition of cadmium, as $CdCl_2$, was done before sterilization to a concentration of 250 μM. After the addition, the pH was adjusted to 6.7-7.

2.2. Analytical determinations

For DW determination, 5 mL samples of culture were filtered through pre-tared Whatman GF/F filter paper (Whatman International Ltd, Maidstone, UK), and the filters were oven-dried overnight at 90 °C, cooled in a desiccator and weighed in an analytical balance. The DW was obtained as the difference between the initial and final weight.

For microscopy images, after 40 h of cellular growth, 0.1 mL of culture medium was collected prior to fluorescence microscopy (Leica DM6000B, Germany). Pictures were taken in differential interference contrast (DIC) with the fluorescence cube TX2 (Ex 560/40 nm; Dicroico 595 nm; Em 645/75 nm).

Cd content in the different samples of *C. sorokiniana* was determined using an Agilent 7700 (Agilent Technologies, Santa Clara, CA, USA) Inductively Coupled Plasma Mass Spectrometry (ICP-MS). Cultures were harvested by centrifugation at 5000×*g* during 5 min, and pellets were lyophilized for 24 h. Thereafter, 0.05 g of dry cells were digested with 1 mL of HNO_3 and 1.5 mL of H_2O_2 in two heat steps in a microwave for 2 min and 350 W and, finally, diluted in Milli-Q water. The standard solution was Multi-element Calibration Standard 2 A from Agilent Technologies (Agilent Technologies, Santa Clara, CA, USA). An external calibration with this multi-element standard was done with concentrations between 1 and 1000 ppb using Sc, Ge, Rh and Tb as internal patron.

2.3. Algal crude extract preparation

C. sorokiniana cells were harvested by centrifugation at the middle of the exponential phase of growth (40 h) and washed three times with Milli-Q water. The cells were resuspended in 50 mM Tris-HCl pH 8.0 buffer at approximately 1 mL of buffer per g of fresh weight, and disrupted by sonication at 4 °C (80 W for 10 cycles of 15 s). The cell debris was centrifuged twice at 14000×*g* for 20 min. The supernatant obtained was used as the crude extract source. Finally, 0.5 mg of proteins were precipitated using the TRIzol method (Jaipal Reddy et al., 2013) for subsequent SWATH-MS analysis.

2.4. Protein relative quantitation by SWATH-MS acquisition and analysis

Protein samples from *C. sorokiniana* 211–32 were alkylated and trypsin-digested as previously described (Vowinckel et al., 2013; García et al., 2019), and SWATH-MS analyses were performed at the Proteomic Facility of the Institute of Plant Biochemistry and Photosynthesis, Seville, Spain.

A data-dependent acquisition (DDA) approach using nano-LC-MS/MS was first performed to generate the SWATH-MS spectral library as described by García et al. (2019). To build the spectral library, the peptide solutions were separated into a nano-LC system (Eksigent, CA, USA) using an Acclaim PepMap C18 column (75 μm Å~25 cm, 3 μm, 100 Å) (Thermo Fisher Scientific). As the peptide eluted, they were injected into a hybrid quadrupole-TOF mass spectrometer TripleTOF 5600+ (Sciex, CA, USA) through a nanospray III ESI source (Sciex) as interface between the nanoLC and the mass spectrometer.

The peptide and protein identifications were performed using Protein Pilot software (version 5.0.1, SCIEX) with the Paragon algorithm. The search was conducted against the Uniprotproteome_Chlorellasorokinianaprotein database (January 2019), specifying iodoacetamide with other possible Cys modifications. The false discovery rate (FDR) was set to 0.01 for both peptides and proteins. The MS/MS spectra of the identified peptides were then used to generate the spectral library for SWATH peak extraction using the add-in for PeakView Software (version 2.1, SCIEX) MS/MSALL with SWATH Acquisition MicroApp (version 2.0, SCIEX). Peptides with a confidence score above 99% (as obtained from the Protein Pilot database search) were included in the spectral library.

For relative quantitation using SWATH analysis, the same samples used to generate the spectral library were analysed using a data-independent acquisition (DIA) method. Each sample (2 μL) was analysed using the LC-MS equipment and LC gradient described above to build the spectral library but instead used the SWATH-MS acquisition method. The method consisted of repeating an acquisition cycle of 34 TOF MS/MS scans (230–1500 m/z, 100 ms acquisition time) of overlapping sequential precursor isolation windows of 25 m/z width (1 m/z overlap) covering the 400–1250 m/z mass range with a previous TOF MS scan (400–1250 m/z, 50 ms acquisition time) for each cycle. The total cycle time was 3.5 s.

The targeted data extraction of the fragment ion chromatogram traces from the SWATH runs was performed by PeakView (version 2.1) with MS/MSALL with SWATH Acquisition MicroApp (version 2.0). This application processed the data using the spectral library created from the shotgun data. Up to 10 peptides per protein and 7 fragments per peptide were selected based on the signal intensity. Any shared and modified peptides were excluded from the processing. Windows of 12 min and 20 mg kg^{-1} width were used to extract the ion chromatograms. SWATH quantitation was attempted for all proteins in the ion library that were identified by Protein Pilot with an FDR below 1%. The extracted ion chromatograms were then generated for each selected fragment ion. The peak areas for the peptides were obtained by summing the peak areas from the corresponding fragment ions. PeakView computed an FDR and a score for each assigned peptide according to the chromatographic and spectral components. Only peptides with an FDR

below 5% were used for protein quantitation. Protein quantitation was calculated by adding the peak areas of the corresponding peptides. To test for differential protein abundance between the two groups, MarkerView (version 1.2.1, SCIEX) was used for signal normalization.

The mass spectrometry proteomics data have been deposited in the ProteomeXchange Consortium via the PRIDE (Vizcaino et al., 2016) partner repository with identifier PXD015932.

3. Results and discussion

3.1. Effect of long-term cadmium exposure on C. sorokiniana growth and morphology

C. sorokiniana was grown in TAP culture medium with increasing concentrations of Cd, ranging from 100 to 250 μM. An untreated culture (Control) was also included (Fig. 1A). During the first 24 h, the growth rate was quite similar in all the Cd concentrations tested. Nevertheless, longer exposure times at a Cd concentration of 250 μM caused a significant inhibition of the growth rate. Thus, for the following experiments, untreated and 250 μM Cd-treated cultures at the middle of the exponential phase (40 h), where there is no limitation of any nutrient, were used to identify the changes that Cd induces in different metabolic pathways and in the morphology of the microalga. At this time, the intracellular Cd concentration calculated by ICP-MS were 2.93 ± 0.06 g Cd · kg DW^{-1}, which shows the bioaccumulation capacity of *C. sorokiniana*. Furthermore, the concentration of Cd in culture medium decreased from 250 ± 7 μM to 145 ± 27 μM, demonstrating that approximately 40% of the Cd in the culture medium was removed at 40 h of Cd exposure.

The morphological differences between *C. sorokiniana* cells cultured in the presence and absence of Cd were analysed by microscopy studies. As shown in Fig. 1B and C, the presence of Cd produced important morphological changes in the microalga. The size and number of vacuoles (Fig. 1C) were considerably higher in Cd-treated cells than in untreated cells, possibly due to the accumulation of this heavy metal. It has been previously reported that the cadmium detoxification mechanisms in plants and microalgae involve transport of the cations to the vacuole, mediated by phytochelatins (Cobbet, 2000). On the other hand, fluorescence microscopic analysis (Fig. 1D and E) showed that the fluorescence of chlorophylls was much higher when the cells were cultured without Cd than with Cd (Fig. 1D), in agreement with the growth results shown in Fig. 1A. Similar results were reported by Carfagna et al. (2013), who showed that *C. sorokiniana* cultured with Cd also exhibited lower photosynthetic activity. All these data suggest that a deeper study is necessary to understand the behaviour of *C. sorokiniana* cells during long-term Cd exposure.

3.2. Proteome alterations in C. sorokiniana due to cadmium exposure

To thoroughly investigate the effect that cadmium provokes on the metabolism and cellular physiology of *C. sorokiniana* and decipher the mechanism of response to this heavy metal, we characterized the protein composition and the relative abundance of most of the microalgal proteins by using SWATH-MS technology.

Protein samples were obtained from *C. sorokiniana* cultures lysed by sonication and precipitated using the TRIzol method as described in section 2.3. Extracted proteins from three biological replicates of untreated and 250 μM Cd-treated cultures were digested, and the peptide solutions were analysed by a shotgun-DDA approach to generate the spectral library. After integrating the six datasets, a total of 13,193 peptides (1% FDR and 96% confidence) and 1776 unique proteins (1% FDR) were identified (Supplemental Dataset 1). For their quantification, the same six biological samples were analysed twice (technical replicas) by a data-independent acquisition (DIA) method using the LC gradient and LC-MS equipment described to generate the spectral library but instead using the SWATH acquisition method described in section 2.4. Therefore, for quantitation, six datasets from untreated and Cd treated cultures were generated and used for the analysis. The fragment spectra were extracted for the twelve runs, and 30,635 ion transitions, 4386 peptides, and 1432 proteins were quantified (Supplemental Dataset 2). A total of 779 of the 1432 proteins quantified had significantly different abundances (p value < 0.05) (Fig. 2A; Table S1). Of these proteins, 218 were more abundant in untreated cultures, exhibiting a fold change >1.5, and 255 were more abundant in Cd-treated cultures, with a fold change <0.66. In addition, 317 proteins were only identified in the control cultures and were below the detection limit in Cd treated cultures (Table S2), and 412 were only identified in the Cd-treated cultures (Table S3).

The 667 proteins that were present or were more abundant in Cd treated cultures were classified by GO according to the UniProt database (Pundir et al., 2016). GO classification in the biological process indicated that 172 proteins fell into the metabolic process classification and 194 into cellular processes including response to stress and DNA damage stimulus (Fig. 2B). The molecular function classification showed that 309 proteins had catalytic activities (Fig. 2C). Analysis of these sets of proteins in KEGG pathway mapping also showed that most of the proteins, 136, were involved in metabolic pathways, mainly in secondary metabolite and amino acid biosynthesis.

An overrepresentation test performed with the PANTHER Classification System showed a 66% enrichment in proteins involved in double-

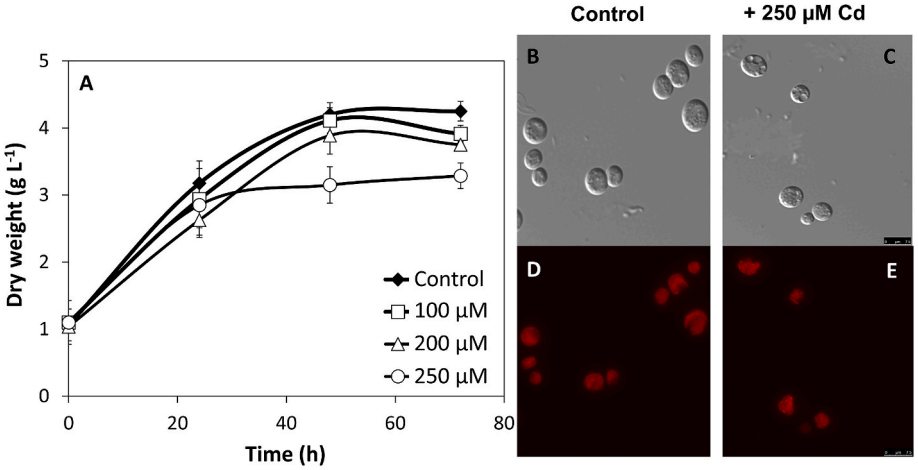

Fig. 1. Physiological effect of Cd in *C. sorokiniana*. (A) Growth curve in the presence of increasing concentrations of Cd. (B–E) Morphological and fluorescence alterations of *C. sorokiniana* cells in the absence (B and D), or presence (C and E) of 250 μM Cd in the culture after 40 h of exposure.

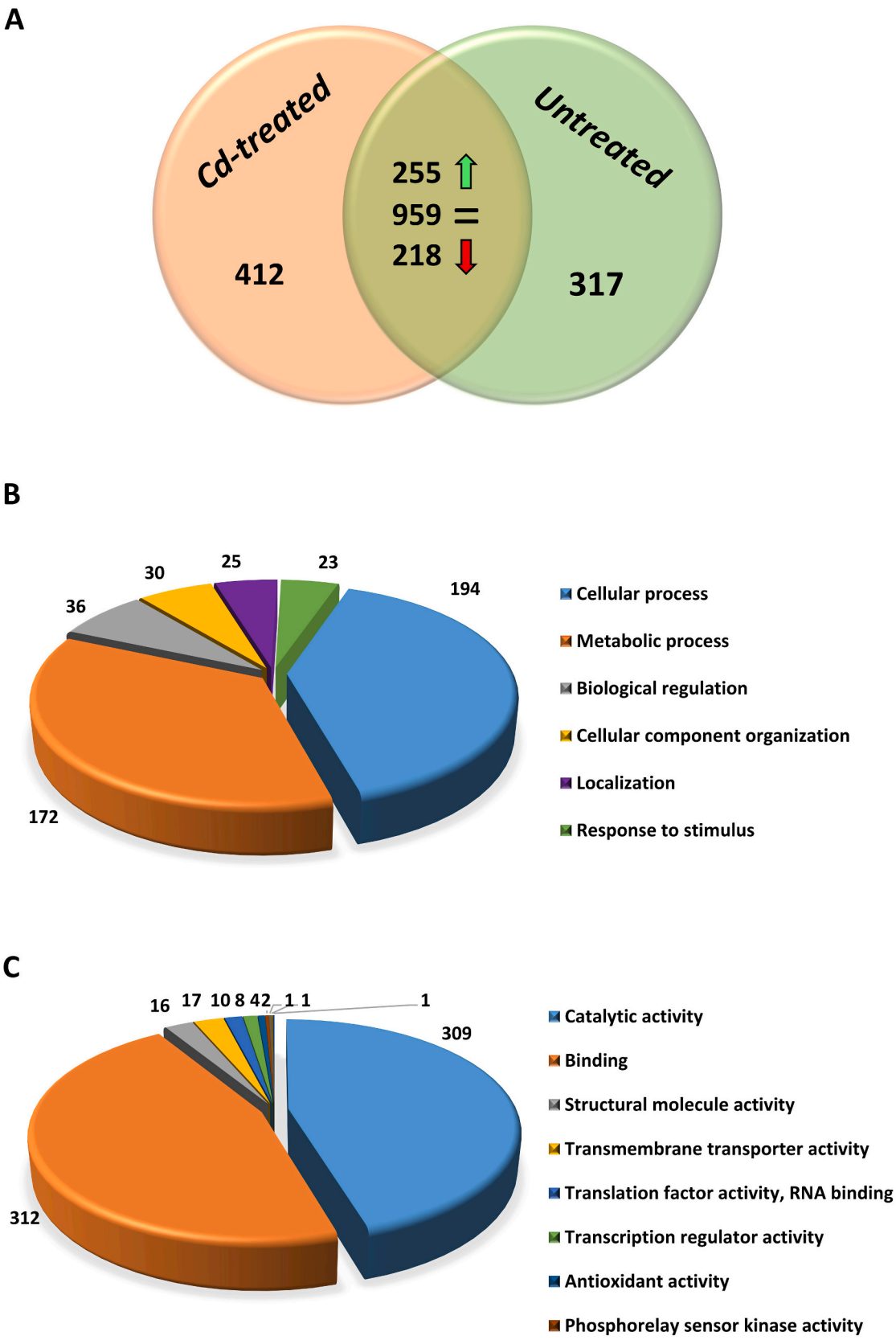

Fig. 2. Venn diagram with the number of proteins identified in untreated and 250 μM Cd-treated *C. sorokiniana* (A) and functional classification of gene ontology (GO) of the proteins that were only present or more abundant in Cd treated cultures categorized by B) Biological processes C) Molecular functions. Of the 1432 proteins quantified in both cultures as described in Material and Methods, 218 were downregulated in Cd cultures (red arrow), 255 were upregulated (green arrow) and 959 did not show significant changes (=). The rest of protein were only identified in untreated or Cd-treated cultures. (For interpretation of the references to colour in this figure legend, the reader is referred to the Web version of this article.)

strand break repair and glutaminyl-tRNAGln biosynthesis such as RAD51 HOMOLOG 1 and 3 (Table S4) (Mi et al., 2017). A subset of proteins involved in Photosystem I assembly also showed a 44% enrichment such as the YCF3-Interacting protein CGL59 orthologue and the protein TAB2 homolog.

Finally, to determine the functional relevance of the effect of Cd on the physiology of *C. sorokiniana*, we used the STRING database v10.5 (Szklarczyk et al., 2015) to analyse the protein-protein interaction network of the protein set that was only present or more abundant in Cd-treated cultures to determine the functional association of those proteins. Using high confidence (interaction score 0.700), a total of 364 protein-protein interactions were observed, and they were significantly enriched (p-value < 0.0362) based on the given protein nodes (Fig. 3). At least three protein clusters that are biologically connected were clearly distinguished after analysis. The first cluster contains a subgroup of proteins involved in metabolic pathways and carbon metabolism (red nodes) linked to a second cluster of the spliceosome and RNA binding (green nodes). The third cluster (blue nodes) comprises a subgroup of ribosomal proteins and predicted proteins of unknown function.

3.3. Cadmium induces proteomic changes in photosynthesis and photorespiration pathways

One of the most important processes in green microalgae is photosynthesis, which has been described as very susceptible to inhibition by heavy metals (Azhar et al., 2019; Shanker et al., 2005). As a consequence, it is important to study how Cd exposure affects this process. Quantitative proteomic profiling in both Cd-treated and untreated *C. sorokiniana* cells revealed that most of the proteins related to photosynthesis were downregulated in the presence of Cd (Fig. 4A, Table 1). This group included ferredoxin (11.7-fold), ferredoxin NADP reductase (1.8-fold), subunits III, VI and XI of the photosystem I reaction center (3.2, 2.0- and 4.2-fold, respectively), whereas a slight upregulation of photosystem II oxygen-evolving enhancer protein 2 (1.6-fold) was observed. Additionally, five antenna proteins were downregulated in Cd cultures, two of them in photosystem I and the other three in

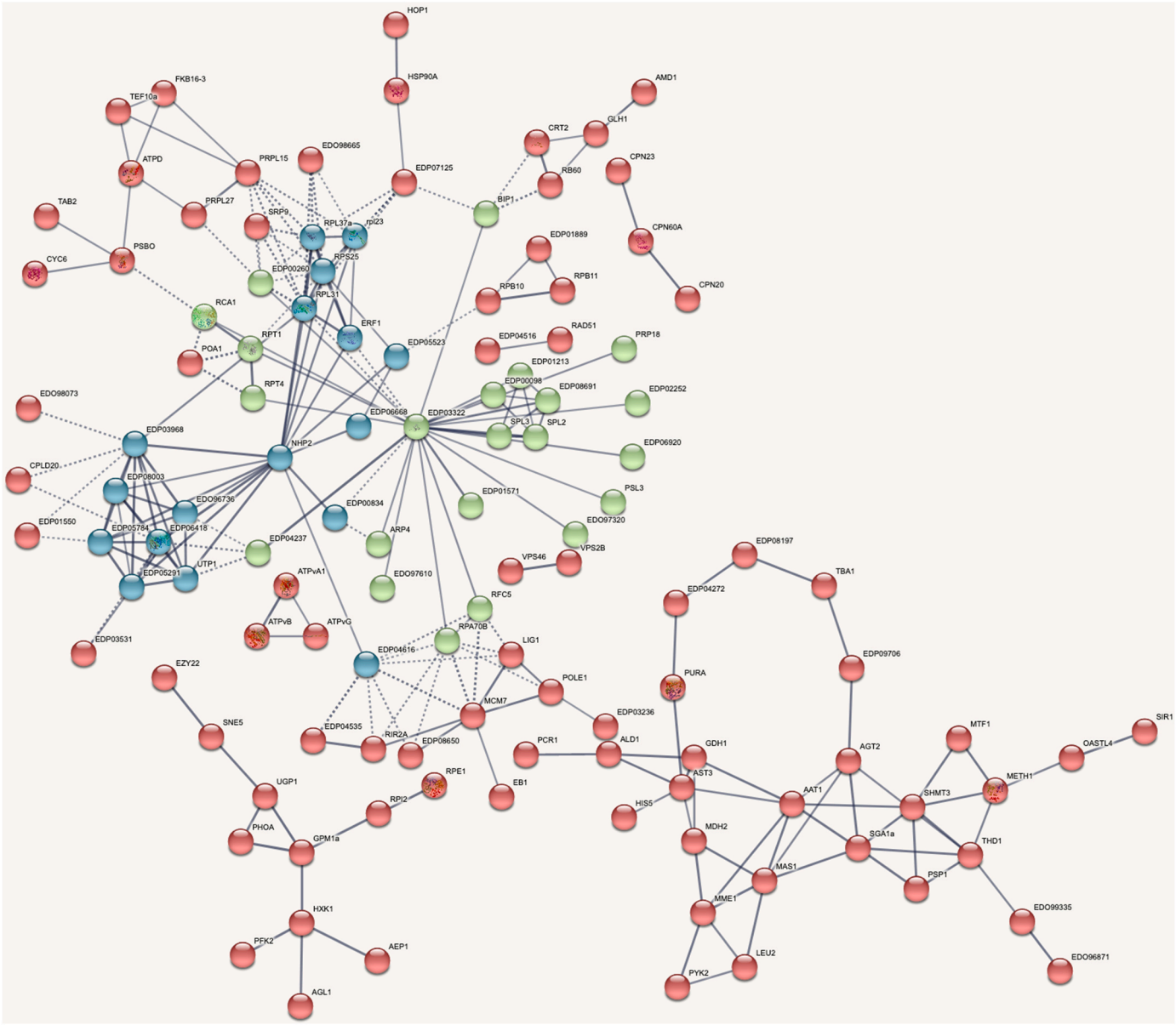

Fig. 3. Protein-protein interaction network of the proteins only present or more abundant in Cd-treated cultures. Round nodes represent proteins, and line edges represent interactions. Dashed lines represent inter-cluster edges. Node modules indicated in red, blue and green colours were identified by k-means clustering. (For interpretation of the references to colour in this figure legend, the reader is referred to the Web version of this article.)

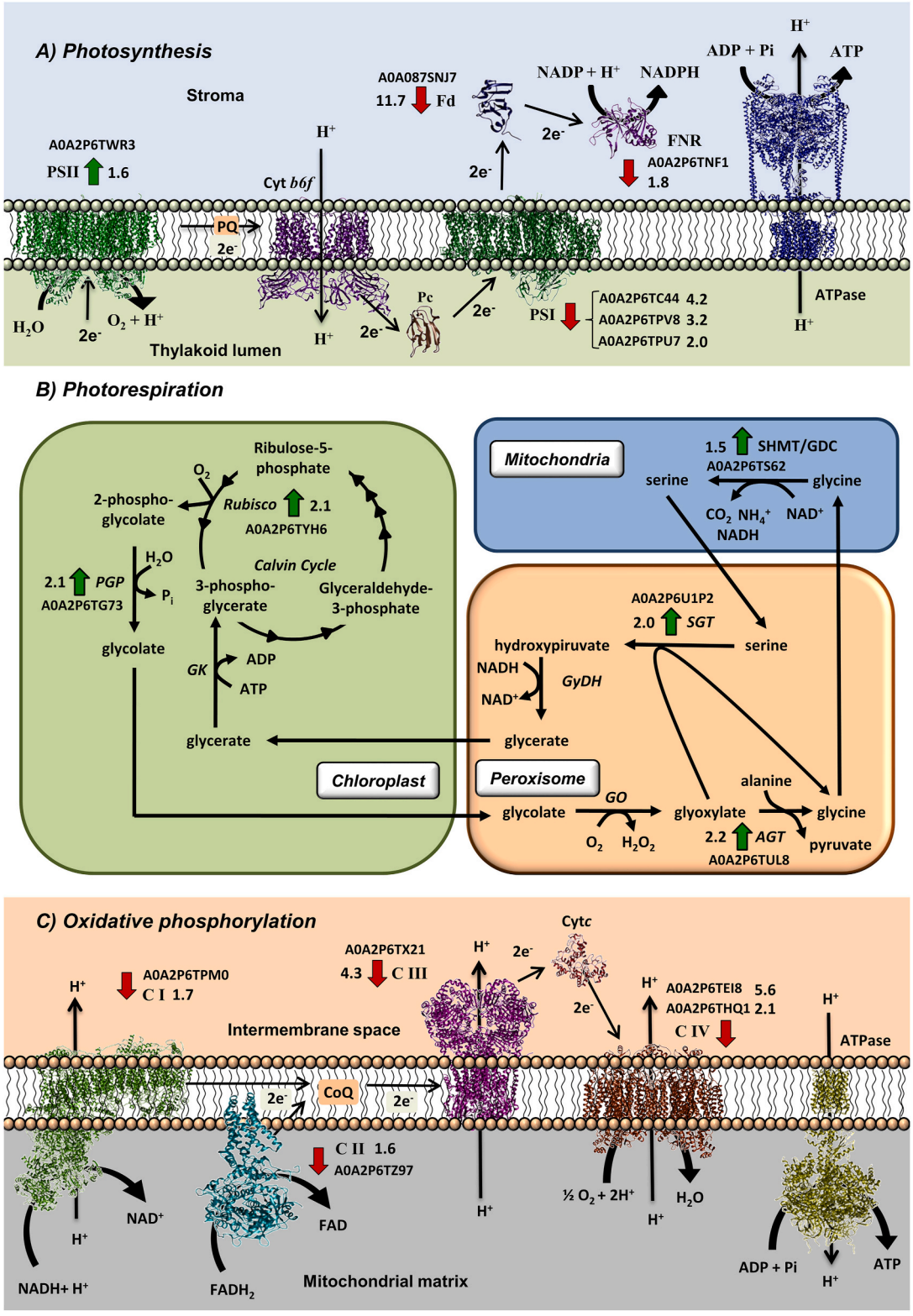

Fig. 4. Effect of Cd on the photosynthesis, photorespiration and oxidative phosphorylation pathways in *C. sorokiniana*. Diagrams of the photosynthesis (A), photorespiration (B) and oxidative phosphorylation (C) pathways are shown, where the upregulated proteins in Cd cultures are represented with green arrows and downregulated proteins with red arrows. The Protein Data Bank (PDB) archives of the 3D structures represented are: 1W5C for photosystem II (PSII), 1Q90 for the cytochrome b6f complex (Cyt b_6f), 6JO5 for photosystem I (PSI), 2PLT for plastocyanin (Pc), 4ITK for ferredoxin (Fd), 3VO1 for ferredoxin-NADP reductase (FNR) and 5Y5Z for ATPase in photosynthesis, and 5LDW for complex I (CI), 4PED for coenzyme Q (CoQ), 1NEN for complex II (CII), 1PPJ for complex III (CIII), 3ZCF for cytochrome c (Cytc), 5B1B for complex IV (CIV) and 2XND for complex V (CV) in oxidative phosphorylation. Photorespiration proteins indicated are: ribulose biphosphate carboxylase/oxygenase (Rubisco), phosphoglycerate phosphatase (PGP), glycolate oxidase (GO), alanine-glyoxylate aminotransferase (AGT), serine hydroxymethyltransferase (SHMT), glycine decarboxylase (GDC), serine-glyoxylate aminotransferase (SGT), glycerate dehydrogenase (GyDH), and glycerate kinase (GK). Accession numbers and fold changes of significant proteins are also showed. (For interpretation of the references to colour in this figure legend, the reader is referred to the Web version of this article.)

Table 1
List of differentially expressed proteins between Cd-treated and untreated cultures categorized by metabolic pathway and described in the text. Red boxes indicate downregulated proteins; green boxes indicate upregulated proteins; and blue boxes indicate proteins only detected in Cd cultures.

Accession	Biological process/Protein name	Fold Change (Average)	p-value
	Photosynthesis		
A0A2P6U1P1	Ferredoxin	11.7	0.00000
A0A2P6TNF1	Ferredoxin-NADP+ reductase	1.8	0.00000
A0A2P6TC44	Photosystem I reaction center subunit XI	4.2	0.00000
A0A2P6TPV8	Photosystem I reaction center subunit III	3.2	0.00003
A0A2P6TPU7	Photosystem I reaction center subunit VI-chloroplastic-like	2.0	0.04897
A0A2P6TWR3	33kDa oxygen evolving of photosystem II	1.6	0.00133
	Photorespiration		
A0A2P6TYH6	Rubisco activase	2.1	0.01862
A0A2P6TG73	Phosphoglycolate phosphatase	2.1	0.00422
A0A2P6TUL8	Alanine--glyoxylate aminotransferase 2-like protein mitochondrial	2.2	0.00046
A0A2P6TS62	Serine hydroxymethyltransferase	1.5	0.00000
A0A2P6U1P2	Serine--glyoxylate aminotransferase isoform A	2.0	0.00000
	Oxidative phosphorilation		
A0A2P6TPM0	Nadh:ubiquinone oxidoreductase complex i intermediate-associated 30	1.7	0.00001
A0A2P6TZ97	Succinate--CoA ligase [ADP-forming] subunit beta, mitochondrial	1.6	0.00001
A0A2P6TX21	Cytochrome b-c1 complex subunit 7	4.3	0.00000
A0A2P6TEI8	Cytochrome c oxidase subunit 6B	5.6	0.00000
A0A2P6THQ1	Mitochondrial cytochrome c oxidase subunit 13 kD	2.1	0.00001
	Stress response		
A0A2P6THP5	Putative lactoylglutathione chloroplastic	2.0	0.00031
A0A2P6TJM0	Lactoylglutathione lyase isoform X2	1.5	0.00001
A0A2P6TZH8	Hydroxyacylglutathione hydrolase	2.1	0.00021
A0A2P6TSG0	Glutatione synthetase	2.1	0.00000
A0A2P6TI90	Glutathione peroxidase	1.2	0.15476
A0A2P6TMT4	Glutathione reductase	1.3	0.00000
A0A2P6TZS9	Glutathione S-transferase isoform B	1.1	0.53137
A0A2P6TNR8	Glutathione S-transferase	1.1	0.48849
A0A2P6TC42	L-ascorbate peroxidase 6	1.8	0.00012
A0A2P6TYS0	Monodehydroascorbate reductase	1.5	0.00001
A0A2P6TUJ2	Catalase	1.7	0.00000

A0A2P6TT94	Heat shock 70 kDa 14-like	1.5	0.00000
A0A2P6TZR3	Heat shock 70 kDa 17	1.3	0.0003
A0A2P6TR21	Heat shock 70	1.5	0.00658
A0A2P6TM18	Heat shock 70	1.2	0.0004
A0A2P6TT53	Heat shock 70B	1.9	0.00000
A0A2P6TSH5	Hsp70-Hsp90 organizing 2		
A0A2P6TX62	Hsp70 nucleotide exchange factor FES1 isoform X1		
A0A2P6TG12	28 kDa heat-and acid-stable phospho-like isoform X1		
	Carbohidrates metabolism		
A0A2P6TZQ3	Acetyl-coenzyme A synthetase	2.2	0.00000
A0A2P6TD11	Pyruvate carboxylase isoform B	2.1	0.00000
A0A2P6TKK3	Pyruvate dehydrogenase E1 component subunit beta-chloroplastic-like	1.7	0.07968
A0A2P6TFS0	Pyruvate, phosphate dikinase	1.4	0.00001
A0A2P6TPT3	Phosphofructokinase family isoform A	1.5	0.01813
A0A2P6TCP5	Glyceraldehyde-3-phosphate dehydrogenase	1.4	0.00000
A0A2P6TBJ6	Phosphoenolpyruvate carboxykinase	1.3	0.01907
A0A2P6U3Z2	Alpha-1,4 glucan phosphorylase	2.3	0.00000
A0A2P6TQG1	Alpha-amylase	1.7	0.0954
A0A2P6TUQ4	4-alpha-glucanotransferase	1.5	0.0484
A0A2P6U2S7	Citrate synthase	1.9	0.00000
A0A2P6TQ82	Fumarate isoform A	1.6	0.00000
A0A2P6TTG2	Succinate dehydrogenase [ubiquinone] iron-sulfur subunit, mitochondrial	1.7	0.00029
A0A2P6U4Q6	Succinate dehydrogenase subunit b560	2.3	0.00000
	N/S metabolism		
A0A2P6V4A3	Glutamate synthase	3.1	0.00000
A0A2P6TJV8	Glutamate dehydrogenase	1.1	0.35633
A0A2P6TQL0	Glutamine synthetase	1.3	0.0003
A0A2P6TEV1	Sulfite reductase isoform A	2.3	0.00000
A0A2P6TE71	Cysteine synthase	1.5	0.00000
A0A2P6TWT6	Serine threonine-phosphatase 2A activator	1.7	0.00651
	Amino acids biosynthesis		
A0A2P6U2U0	Serine hydroxymethyltransferase	1.8	0.00000
A0A2P6TS62	Serine hydroxymethyltransferase	1.5	0.00000

A0A2P6U422	Serine hydroxymethyltransferase	1.1	0.50462
A0A2P6U2V8	Alanine aminotransferase 2	1.5	0.00000
A0A2P6TJZ5	Alanine aminotransferase isoform B	1.6	0.00000
A0A2P6TUL8	Alanine--glyoxylate aminotransferase 2-like protein mitochondrial	2.2	0.00046
A0A2P6TYD7	Phosphoserine phosphatase	1.8	0.00056
A0A2P6U101	Serine/threonine-protein phosphatase	2.5	0.00000
A0A2P6TWE7	Aspartate aminotransferase	2.3	0.00000
A0A2P6TPG2	Pyrroline-5-carboxylate reductase	1.7	0.00000
A0A2P6TUJ0	Aldehyde dehydrogenase 22A1	3.8	0.00551
A0A2P6TEC8	Aldehyde dehydrogenase	2.4	0.00000
	Lipids/Carotenoids metabolism		
A0A2P6TKW3	Plastid acyl-ACP desaturase	5.6	0.00000
A0A2P6TEE4	Zeaxanthin epoxidase	1.7	0.03449
A0A2P6TFB0	Zeta-carotene desaturase	2.5	0.00000

photosystem II. These results show a general downregulation in photosynthesis, and the inhibition of chlorophyll production, which is consistent with the information obtained from fluorescence microscopy (Fig. 1D and E). The microscopic images showed that *C. sorokiniana* cells cultured in the presence of Cd had lower red fluorescence due to the lower chlorophyll content, and consequently, they should have lower photosynthetic activity. Additionally, these results were in agreement with previous physiological reports on different plants and microalgae (Ma et al., 2018), which show that the photosynthetic system is affected by this heavy metal.

Moreover, the photorespiration pathway, which involves the oxygenation of ribulose 1,5-biphosphate by Rubisco, was upregulated in the presence of Cd. Although photorespiration consumes ATP and reducing equivalents, it has been proposed as an adaptation mechanism that plants usually adopt under photoinhibition conditions when the photosynthetic electron transport chain is diminished. Moreover, this process provides other metabolites such as glycine, which is essential in glutathione (GSH) and phytochelatin (PC) synthesis during metallic stress (D'Alessandro et al., 2013). In this proteomic study, most proteins related to photorespiration were upregulated when *C. sorokiniana* was cultured in the presence of Cd. Fig. 4B and Table 1 show that Rubisco (2.1-fold), phosphoglycerate phosphatase (2.1-fold), alanine-glyoxylate aminotransferase (2.2-fold), serine hydroxymethyltransferase (1.5-fold) and serine-glyoxylate aminotransferase (2.0-fold) were significantly upregulated. These data are in accordance with previous physiological results obtained when *C. sorokiniana* was cultivated in the presence of moderate amounts of Cd (Carfagna et al., 2013) and with previous proteomics results obtained in *Skeletonema dohrnii* (Thangaraj et al., 2019).

3.4. Responses of cellular respiration to cadmium treatment

Exposure of *C. sorokiniana* to cadmium caused a general downregulation of the main respiratory chain components (Fig. 4C, Table 1), with complexes I, II and III being some the most affected (1.7-, 1.6- and 4.3-fold, respectively). Nevertheless, complex V (ATP synthase) was not affected by long-term exposure to Cd. It is interesting to note that this downregulation was related to the upregulation of photorespiration (Fig. 4B), which was strongly induced in the presence of this heavy metal; because both processes have to compete for the available O_2 in cells. Furthermore, it has been reported that this competition could produce hypoxia in mitochondria, which reduces respiratory activity (Gupta et al., 2009). Finally, there was also a downregulation of subunit 6 b of complex IV (Cytochrome *c* oxidase; 5.6-fold). This alteration in complex IV together with the downregulation of complex III (Cytochrome bc_1 complex) could cause the accumulation of reactive oxygen species (ROS), as has been described in the microalga *Thalasiossira pseudonana*, where the induction of different antioxidant mechanisms due to the alteration of normal cell homeostasis has been observed (Lin et al., 2017).

3.5. Cadmium provokes oxidative stress and alterations in antioxidant defences

To mitigate the toxic effect of ROS, plant cells have developed different mechanisms to regulate the amount of these compounds that they produce. The initial response to oxidative stress is related to changes in the glutathione-ascorbate cycle and catalase activity, which are responsible for the degradation of H_2O_2. Moreover, a non-enzymatic response to heavy metals, including reduced glutathione or phytochelatins synthesis, is developed (Gill and Tuteja, 2010). We found that the production of GSH is enhanced through the upregulation of the enzymes lactoglutathione chloroplastic, lactoylglutathione lyase, hydroxyacylglutathione hydrolase and glutathione synthetase, which increased 2.0-, 1.5-, 2.1- and 2.1-fold, respectively (Table 1). Additionally, glutathione peroxidase, glutathione reductase and glutathione S transferase were slightly upregulated in Cd cultures (1.2-, 1.3- and 1.1-fold, respectively). Moreover, in the glutathione-ascorbate cycle, the enzymes L-ascorbate peroxidase and monodehydroascorbate reductase were upregulated (1.8- and 1.5-fold, respectively). Finally, the only catalase detected followed the tendency of the other antioxidant proteins (1.7-fold). These results are in agreement with previous physiological and proteomics studies, where the antioxidant system is upregulated when different heavy metals are present in the environment of microalgae and plants (Ismaiel and Said, 2018; Du et al., 2018; Rihab et al., 2016).

Another antioxidant strategy in green microalgae and plants is the repair of damaged proteins. As part of this response, cells induce the synthesis of a group of proteins called heat shock proteins (HSPs), which function as chaperones to maintain cellular homeostasis (Hasan et al.,

2017). These proteins are able to promote cellular redox homeostasis through stimulating antioxidant systems and to prevent protein aggregation under stress conditions. In addition, most HSPs are strongly inducible and some are constitutively expressed under environmental stress conditions (Mu et al., 2013). Most of the HSPs detected in the *C. sorokiniana* proteome were upregulated in Cd cultures, and some of them were only detected under these conditions (Tables 1, S1 and S3). This result correlates with the data of Sewelam et al. (2019), who reported that the expression of HSPs in *Arabidopsis thaliana* under non-stress conditions is very low.

Although the induction of the glutathione-ascorbate cycle and increased HSPs expression are the first responses to ROS, there are additional protective mechanisms usually employed to combat the oxidative stress. Consequently, other metabolic pathways, including nutrient assimilation, will be altered, being their study very important.

3.6. Effect of cadmium on carbon assimilation and metabolism

The main carbon source when *C. sorokiniana* is cultured in TAP medium is acetate, which is assimilated and converted to acetyl-CoA by acetyl-CoA synthetase (ACS). In the chlorophyte *Chlamydomonas reinhardtii*, expression of the gene encoding ACS has been reported to be induced when the concentration of the carbon source increases (Rengel et al., 2018).

In this study, the culture medium had a concentration of 100 mM acetate, which is in excess of the carbon needs of the microalga (León-Vaz et al., 2019). However, ACS was downregulated (2.2-fold) in the presence of Cd (Fig. 5, Table 1), causing a limitation in the carbon supply via acetate. As a result, microalgae should use an alternative carbon source. Accordingly, phosphoenolpyruvate carboxykinase, the enzyme that catalyses the transformation from oxaloacetate to phosphoenolpyruvate, was slightly upregulated (1.3-fold). This observation is in accordance with a possible activation of gluconeogenesis to supply glucose as a carbon source. Moreover, there was an upregulation of the first steps of glycolysis in the presence of Cd, but without statistically significant differences (Fig. 5, Table 1). Only phosphofructokinase and pyruvate dehydrogenase exhibited a significant upregulation (1.5- and 1.7-fold) in Cd cultures, whereas the downregulated expression of glyceraldehyde 3-phosphate dehydrogenase without statistically significant differences (1.4-fold) was observed. On the other hand, α-1, 4-glucanphosphorylase (2.3-fold), α-amylase (1.7-fold), and 4-α-glucanotransferase (1.5-fold) involved in starch catabolism to produce glucose were upregulated by Cd stress. This effect can be explained as an adaptation mechanism, because the intracellular glucose stores and the glucose produced by gluconeogenesis are the more efficient sources of carbon during Cd stress conditions when the microalga is cultivated with acetate as a carbon source.

Finally, a slight downregulation in the tricarboxylic acid (TCA) cycle was observed when *C. sorokiniana* was cultured under stress conditions (Fig. 5, Table 1). Significant differences existed in the expression of citrate synthase (1.9-fold), fumarase (1.6-fold) and succinate dehydrogenase (2.3 and 1.7-fold). These results show that the TCA cycle does not present important alterations when *C. sorokiniana* is cultured with Cd, in agreement with recent studies in plants or clams (He et al., 2019; Ji et al., 2019). This unaltered effect may occur in order to maintain the supply of reducing power during Cd exposure. Furthermore, under these conditions, some subunits of pyruvate dehydrogenase were also upregulated, which supports this postulate. In addition, the slight upregulation of carbohydrate metabolism in Cd cultures has been reported previously in *Brassica parachinensis* (Zhou et al., 2019).

3.7. Cadmium causes changes in nitrogen and sulphur assimilation and metabolism

C. sorokiniana was cultured using ammonium as nitrogen source. This N-source is preferred for microalgae and can be assimilated through the glutamine synthetase/glutamate synthase (GS/GOGAT) cycle, as well as through the alternative pathway of the amination of 2-oxoglutarate catalysed by NAD(P) glutamate dehydrogenase (GDH) (Vega, 2019). In this proteomic study, upregulation of glutamate biosynthesis produced by Cd was observed, mainly in the case of GOGAT (3.1-fold) and slightly in the case of GS (1.3-fold) (Fig. 5; Table 1). Alternatively, the production of glutamate was also slightly upregulated via GDH (1.1-fold). This upregulation of GDH detected agrees with previous studies, which described an increase in GDH activity levels during different abiotic stresses, such as Cd treatment, high salinity, high light and the presence of ammonium in *Chlamydomonas reinhardtii* (Domínguez et al., 2003). Moreover, GDH plays a central role in the re-assimilation of ammonia produced by photorespiration (Miflin and Habash, 2002) which, together with the upregulation of the photorespiration pathway observed (Fig. 4B), supports the upregulation of GDH described in this study.

On the other hand, sulphur is another essential macronutrient for microalgae. We observed that the S assimilation pathway was also mainly upregulated (Fig. 5, Table 1) by Cd stress. Sulphite reductase (2.3-fold), which catalyses the reduction of sulphite to sulphur, and O-acetylserine (thiol)lyase (OASTL; cysteine synthase) (1.5-fold), which is involved in the biosynthesis of cysteine, were upregulated by Cd, while enzymes involved in the reduction of sulphate to sulphite did not present significant differences. It was shown that the presence of Cd in culture medium can increase the sulphate uptake rate in *Chlamydomonas reinhardtii* by 40% (Vega et al., 2006). In addition, an increase in the amount of cysteine and glutamate required for the synthesis of phytochelatins (PCs) induced by Cd stress, has been reported (Morelli and Scarano, 2004). All these previous data support the upregulation observed in N and S metabolism under Cd stress.

3.8. Cadmium produces alterations in the synthesis of amino acids

Alterations in N and S metabolism could influence the production of different amino acids (AAs). Thus, it would be interesting to study those whose synthesis is up- or downregulated when *C. sorokiniana* is cultured in the presence of Cd. The results showed, as was previously mentioned, an upregulation by Cd of enzymes involved in glutamate and cysteine synthesis (Table 1). In addition, the production of glycine and serine was altered when *C. sorokiniana* was under Cd stress. Serine hydroxymethyltransferase (1.8-, 1.5- fold), alanine aminotransferase (1.6-fold) and alanine-glyoxylate aminotransferase (2.2-fold), which contribute to glycine production, were upregulated. Glycine, together with glutamate and cysteine, is required for GSH and PC synthesis, as a response to Cd stress (Cobbett, 2000). On the other hand, phosphoserine phosphatase and serine/threonine phosphatase were also upregulated (1.8- and 2.5-fold, respectively). These enzymes are involved in the production of serine, which is needed for the synthesis of cysteine and glycine, and supports glutathione synthesis (Zhou et al., 2017). In addition, recent transcriptomics studies have reported the upregulation and crucial role of serine/threonine phosphatase in microalgae under oxidative stress (Zhang et al., 2018).

The production of glutamate was also upregulated via aspartate to glutamate and proline to glutamate. The first process is catalysed by aspartate aminotransferase, which showed a higher level in Cd cultures than in those without Cd (2.3-fold). In the second process, the involved enzymes were also upregulated, such as pyrroline-5-carboxylate reductase (1.7-fold) and two aldehyde dehydrogenases (3.8 and 2.4-fold). These data, together with the upregulated enzymes studied in section 3.7 for the synthesis of glutamate and cysteine, suggest the crucial role of PCs during Cd stress, which are responsible of transporting Cd^{2+} to vacuoles as a detoxification mechanism (Gill and Tuteja, 2010).

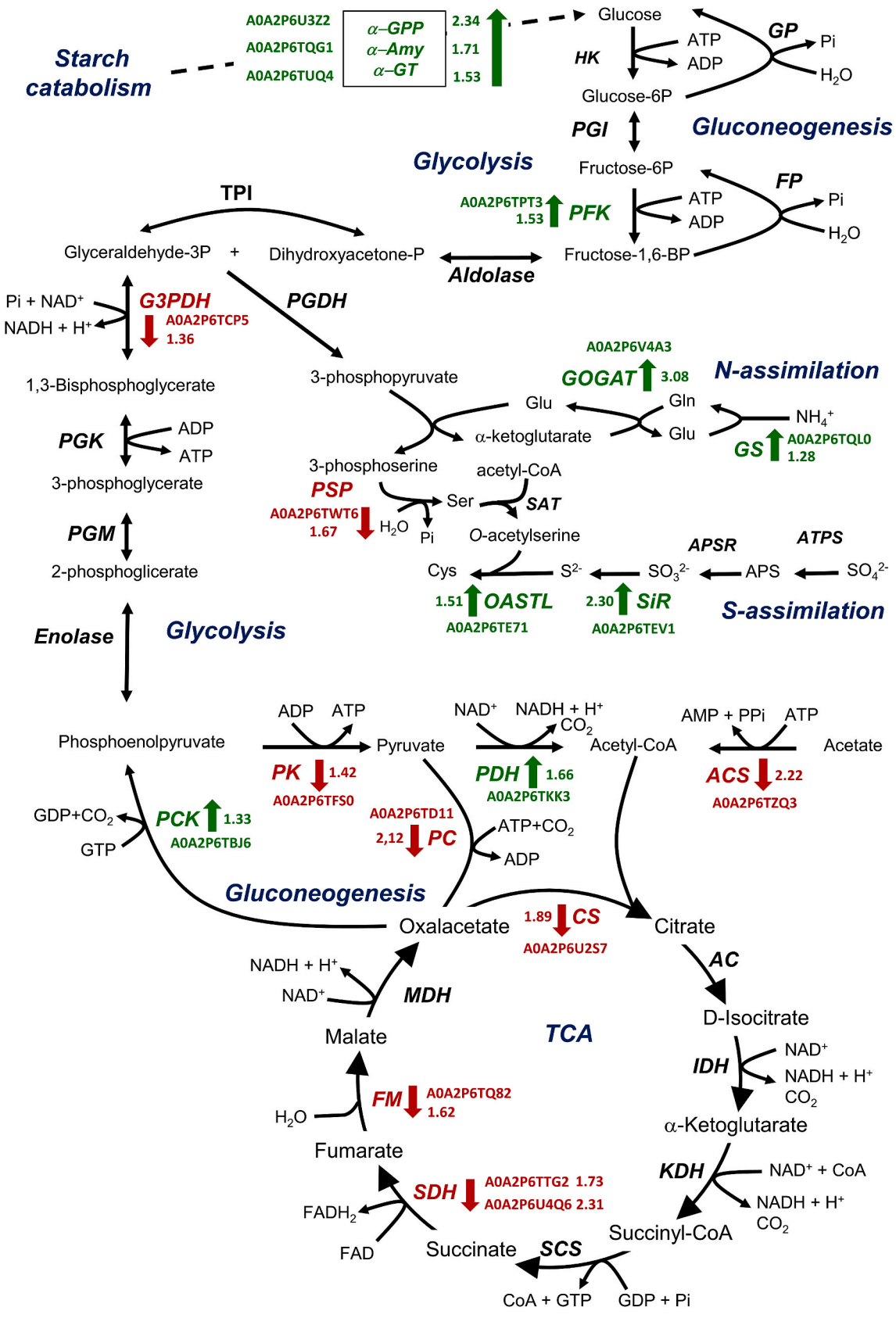

(caption on next page)

Fig. 5. Alterations in starch catabolism, glycolysis, gluconeogenesis TCA cycle and N and S assimilation metaolism in *C. sorokiniana* after Cd exposure. Schemes of starch catabolism, glycolysis, gluconeogenesis and the TCA cycle are shown, where upregulated proteins are represented with green arrows and downregulated with red arrows. Proteins represented are α-1,4 glucanphosphorylase (α-GPP), α-amylase (α-Amy) and 4-α-glucanotransferase (α-GT) for starch catabolism; hexokinase (HK), glucose 6-phosphate isomerase (PGI), 6-phosphofructokinase (PFK), aldolase, triose phosphate isomerase (TPI), glyceraldehyde 3-phosphate dehydrogenase (G3PDH), phosphoglycerate kinase (PGK), phosphoglycerate mutase (PGM), enolase, pyruvate kinase (PK), pyruvate dehydrogenase (PDH) and acetyl CoA synthetase (ACS) for glycolisis; pyruvate carboxylase (PC), pyruvate carboxykinase (PCK), fructose-1,6-biphosphatase (FP) and glucose 6-phosphatase (GP) for gluconeogenesis; citrate synthase (CS), actinase (AC), isocitrate dehydrogenase (IDH), α-ketoglutarate dehydrogenase (KDH), succinyl CoA synthase (SCS), succinate dehydrogenase (SDH), fumarase (FM), and malate dehydrogenase (MDH) for the TCA cycle; glutamine synthetase (GS), glutamate synthase (GOGAT), phosphoglycerate dehydrogenase (PGDH), phosphoserine transaminase (PSAT), and phosphoserine phosphatase (PSP) in N metabolism, and ATP-sulfurylase (ATPS), adenosine-phosphosulfate reductase (APSR), sulphite reductase (SiR), O-acetylserine (thiol)lyase (OASTL) and serine acetyltransferase (SAT) in S metabolism. Accession numbers and fold changes of significant proteins are also showed. (For interpretation of the references to colour in this figure legend, the reader is referred to the Web version of this article.)

3.9. Effect of cadmium on ribosomal proteins

Ribosomes play a central role in protein metabolism. In this work, 30 proteins related to ribosomes were found to be downregulated in Cd cultures (Fig. 3, Table. S1), while 9 of them, fundamentally in the large subunit, were upregulated (Table. S1). These variations in the expression of ribosomal proteins could produce a decrease in the concentration of proteins in *C. sorokiniana* under stress conditions, which is in agreement with the lower protein content obtained in crude extracts prepared from Cd cultures (data not shown). Moreover, recent transcriptomics studies in plants and green microalgae have also shown the downregulation of ribosome proteins, when they are cultured with Cd (Zhu et al. 2018, 2019), although these studies do not differentiate between large and small subunits.

3.10. Other changes induced by cadmium

There are other metabolic pathways that are very susceptible to regulation in abiotic stress, such as the biosynthesis of lipids and carotenoids (Couso et al., 2012; Rengel et al., 2018). In this proteomic study, a remarkable upregulation of the plastid acyl-ACP desaturase (5.6-fold), which participates in the synthesis of polyunsaturated fatty acids, was observed during Cd stress (Table 1). However, there was a general downregulation of glycerolipid biosynthesis under these conditions (Table. S1, S2). This response is in agreement with the morphology of the *C. sorokiniana* cells under Cd treatment (Fig. 1C and E). The downregulation of these proteins could be the cause of alterations in the structures of membrane cells, as has been reported in *Euglena gracilis* (Einicker-Lamas et al., 1996) during Cd-exposure stress.

On the other hand, the proteomic study did not reveal much information about the enzymes of the carotenogenic pathway, with zeaxanthin epoxidase (ZEP) and zeta-carotene desaturase (ZDS) showing the most important differences. The downregulation of ZEP (1.7-fold), an enzyme that catalyses the conversion of zeaxanthin to violaxanthin, could induce the accumulation of zeaxanthin, which is a typical response to oxidative stress in microalgae (Varela et al., 2015). Using protein synthesis inhibitors, we have previously observed in *Chlamydomonas reinhardtii*, that the biosynthesis of zeaxanthin is upregulated by stressing conditions, such as high irradiance and nitrogen starvation (Couso et al., 2012). Interestingly, the present study did not reveal the induction by Cd of violaxanthin de-epoxidase, the reverse enzyme of the xanthophyll cycle. ZDS, also downregulated by Cd stress (2.5-fold), is involved in the desaturation of phytoene, which is subjected to the sequential action of phytoene (PDS) and ZDS, producing all-trans lycopene. ZDS and PDS share a common reaction mechanism: both have plastoquinone (PQ) as the hydrogen acceptor, connecting this pathway with the photosynthetic electron transport chain (Grossman et al., 2004). In the presence of Cd, the downregulation of photosynthesis (Fig. 4A) might exceed the rate of oxidation of plastoquinol to regenerate PQ, causing a low availability of oxidized PQ and, consequently, a downregulation of this enzyme. Similar results in transcriptome analysis were reported in *Euglena gracilis* under stress conditions (Kato et al., 2019).

4. Conclusions

The results reported in this work reveal that the microalga *C. sorokiniana* is highly tolerant to Cd. Nevertheless, this heavy metal causes important alterations in the morphology and protein composition of microalgae. This study reveals that Cd provokes an increase in the number and size of vacuoles. Moreover, the proteomic study shows a downregulation in certain processes, such as photosynthesis and oxidative phosphorylation, which are essential for the production of ATP, and an upregulation of photorespiration. The main supply of carbon under Cd stress may come from starch degradation and gluconeogenesis, while N and S assimilation are upregulated in order to produce glutamate and cysteine, which are necessary for chelation of Cd. There is also an upregulation of antioxidant enzymes and HSPs by Cd. Finally, this study demonstrates that the synthesis of AAs and ribosomal function are highly altered, causing a decrease in the amount of total protein in Cd cultures. However, the microalga can survive at 250 μM of this heavy metal due to the profound adaptation of its physiology that occurs, which makes *C. sorokiniana* a potential microorganism for the development of bioremediation processes.

Credit author statement

Antonio León-Vaz: conceptualization, investigation and methodology; Luis C. Romero: conceptualization, methodology and writing – review; Cecilia Gotor: review; Rosa León: writing – review and funding acquisition; Javier Vigara: conceptualization; writing - review and editing.

Declaration of competing interest

The authors declare that they have no known competing financial interests or personal relationships that could have appeared to influence the work reported in this paper.

Acknowledgements

This work was supported by European governments (INTERREG VA-POCTEP- 2014–2020; 0055_ALGARED_PLUS_5_E) and the European Regional Development Fund through the Agencia Estatal de Investigación grants (PID 2019-109785 GB-I00 and PID 2019-110438RB-C22). We want to thank Dr. Rocío Rodríguez for the proteomics service.

Appendix A. Supplementary data

Supplementary data to this article can be found online at https://doi.org/10.1016/j.ecoenv.2020.111301.

References

Ahsan, N., Renaut, J., Komatsu, S., 2009. Recent developments in the application of proteomics to the analysis of plant responses to heavy metals. Proteomics 9, 2602–2621. https://doi.org/10.1002/pmic.200800935.

Akhtar, N., 2004. Removal and recovery of nickel(II) from aqueous solution by loofa sponge-immobilized biomass of *Chlorella sorokiniana*: characterization studies. J. Hazard Mater. 108, 85–94. https://doi.org/10.1016/j.jhazmat.2004.01.002.

Akhtar, N., Iqbal, M., Zafar, S.I., Iqbal, J., 2008. Biosorption characteristics of unicellular green alga *Chlorella sorokiniana* immobilized in loofa sponge for removal of Cr (III). J. Environ. Sci. 20, 231–239. https://doi.org/10.1016/s1001-0742(08)60036-4.

Ali, H., Khan, E., Sajad, M.A., 2013. Phytoremediation of heavy metals: concepts and applications. Chemosphere 91, 869–881. https://doi.org/10.1016/j.chemosphere.2013.01.075.

Alqadami, A.A., Khan, M.A., Otero, M., Siddiqui, M.R., Jeon, B.-H., Batoo, K.M., 2018. A magnetic nanocomposite produced from camel bones for an efficient adsorption of toxic metals from water. J. Clean. Prod. 178, 293–304. https://doi.org/10.1016/j.jclepro.2018.01.023.

Anand, V., Singh, P.K., Banerjee, C., Shukla, P., 2017. Proteomic approaches in microalgae: perspectives and applications. 3 Biotech 7. https://doi.org/10.1007/s13205-017-0831-5.

Aroca, A., Benito, J.M., Gotor, C., Romero, L.C., 2017. Persulfidation proteome reveals the regulation of protein function by hydrogen sulfide in diverse biological processes in *Arabidopsis*. J. Exp. Bot. 68, 4915–4927. https://doi.org/10.1093/jxb/erx294.

Azhar, M., Zia urRehman, M., Ali, S., Qayyum, M.F., Naeem, A., Ayub, M.A., Anwar ulHaq, M., Iqbal, A., Rizwan, M., 2019. Comparative effectiveness of different biochars and conventional organic materials on growth, photosynthesis and cadmium accumulation in cereals. Chemosphere 227, 72–81. https://doi.org/10.1016/j.chemosphere.2019.04.041.

Carfagna, S., Lanza, N., Salbitani, G., Basile, A., Sorbo, S., Vona, V., 2013. Physiological and Morphological Responses of Lead or Cadmium Exposed *Chlorella Sorokiniana* 211-8K (Chlorophyceae), vol. 2. Springer Plus, pp. 1–7.

Cobbet, C., 2000. Phytochelatins and their roles in heavy metal detoxification. Plan tPhysiol 123, 825–832. https://doi.org/10.1104/pp.123.3.825.

Couso, I., Vila, M., Vigara, J., Cordero, B.F., Vargas, M.Á., Rodríguez, H., León, R., 2012. Synthesis of carotenoids and regulation of the carotenoid biosynthesis pathway in response to high light stress in the unicellular microalga *Chlamydomonas reinhardtii*. Eur. J. Phycol. 47, 223–232. https://doi.org/10.1080/09670262.2012.692816.

D'Alessandro, A., Taamalli, M., Gevi, F., Timperio, A.M., Zolla, L., Ghnaya, T., 2013. Cadmium stress responses in *Brassica juncea*: hints from proteomics and metabolomics. J. Proteome Res. 12, 4979–4997. https://doi.org/10.1021/pr400793e.

Dixit, R., Wasiullah, E., Malaviya, D., Pandiyan, K., Singh, U., Sahu, A., Shukla, R., Singh, B., Rai, J., Sharma, P., Lade, H., Paul, D., 2015. Bioremediation of heavy metals from soil and aquatic environment: an overview of principles and criteria of fundamental processes. Sustainability 7, 2189–2212. https://doi.org/10.3390/su7022189.

Domínguez, M.J., Gutiérrez, F., León, R., Vilchez, C., Vega, J.M., Vigara, J., 2003. Cadmium increases the activity levels of glutamate dehydrogenase and cysteine synthase in *Chlamydomonas reinhardtii*. Plant Physiol. Biochem. 41, 828–832. https://doi.org/10.1016/s0981-9428(03)00114-1.

Du, H., Liang, H., Jiang, Y., Qu, X., Yan, H., Liu, X., 2018. Proteome responses of *Gracilaria lemaneiformis* exposed to lead stress. Mar. Pollut. Bull. 135, 311–317. https://doi.org/10.1016/j.marpolbul.2018.07.030.

Einicker-Lamas, M., Soares, M.J., Soares, M.S., Oliveira, M.M., 1996. Effects of cadmium on *Euglena gracilis* membrane lipids. Braz. J. Med. Biol. Res. 29 (8), 941–948.

Gao, J., Qiu, Y., Hou, B., Zhang, Q., Zhang, X., 2018. Treatment of wastewater containing nickel by complexation- ultrafiltration using sodium polyacrylate and the stability of PAA-Ni complex in the shear field. Chem. Eng. J. 334, 1878–1885. https://doi.org/10.1016/j.cej.2017.11.087.

García, I., Arenas-Alfonseca, L., Moreno, I., Gotor, C., Romero, L.C., 2019. HCN regulates cellular processes through posttranslational modification of proteins by S-cyanylation. Plant Physiol. 179, 107–123. https://doi.org/10.1104/pp.18.01083.

Gill, S.S., Tuteja, N., 2010. Reactive oxygen species and antioxidant machinery in abiotic stress tolerance in crop plants. Plant Physiol. Biochem. (Paris) 48, 909–930. https://doi.org/10.1016/j.plaphy.2010.08.016.

Grossman, A.R., Lohr, M., Im, C.H., 2004. *Chlamydomonas reinhardtii* the landscape of pigments. Annu. Rev. Genet. 38, 119–173. https://doi.org/10.1146/annurev.genet.38.072902.092328.

Gupta, K.J., Zabalza, A., van Dongen, J.T., 2009. Regulation of respiration when the oxygen availability changes. Physiol. Plantarum 137, 383–391. https://doi.org/10.1111/j.1399-3054.2009.01253.x.

Gutsch, A., Keunen, E., Guerriero, G., Renaut, J., Cuypers, A., Hausman, J.F., Sergeant, K., Luo, Z.B., 2018. Long-term cadmium exposure influences the abundance of proteins that impact the cell wall structure in *Medicago sativa* stems. Plant Biol. 20, 1023–1035. https://doi.org/10.1111/plb.12865.

Harris, E., 2009. The Chlamydomonas sourcebook, 2nded.

Hasan, M.K., Cheng, Y., Kanwar, M.K., Chu, X.-Y., Ahammed, G.J., Qi, Z.-Y., 2017. Responses of plant proteins to heavy metal stress: a review. Front. Plant Sci. 8 (1492), 1–16. https://doi.org/10.3389/fpls.2017.01492.

He, L., Jing, Y., Shen, J., Li, X., Liu, H., Geng, Z., Wang, M., Li, Y., Chen, D., Gao, J., Zhang, W., 2019. Mitochondrial pyruvate carriers prevent cadmium toxicity by sustaining the TCA cycle and glutathione synthesis. Plant Physiol. 180, 198–211. https://doi.org/10.1104/pp.18.01610.

Ismaiel, M.M.S., Said, A.A., 2018. Tolerance of *Pseudochlorella pringsheimii* to Cd and Pb stress: role of antioxidants and biochemical contents in metal detoxification. Ecotoxicol. Environ. Saf. 164, 704–712. https://doi.org/10.1016/j.ecoenv.2018.08.088.

Izadpanah, M., Gheshlaghi, R., Mahdavi, M.A., Elkamel, A., 2018. Effect of light spectrum on isolation of microalgae from urban wastewater and growth characteristics of subsequent cultivation of the isolated species. Algal Res 29, 154–158. https://doi.org/10.1016/j.algal.2017.11.029.

Jaipal Reddy, P., Rao, A.A., Malhorta, D., Sharma, S., Kumar, R., Jain, R., Gollapalli, K., Pendharkar, N., Rapole, S., Srivastava, S., 2013. A simple protein extraction method for proteomic analysis of diverse biological specimens. Curr. Proteonomics 10, 298–311. https://doi.org/10.2174/15701646113106660004.

Ji, C., Lu, Z., Xu, L., Li, F., Cong, M., Shan, X., Wu, H., 2019. Evaluation of mitochondrial toxicity of cadmium in clam *Ruditapes philippinarum* using iTRAQ-based proteomics. Environ. Pol. 251, 802–810. https://doi.org/10.1016/j.envpol.2019.05.046.

Kato, S., Tanno, Y., Takaichi, S., Shinomura, T., 2019. Low temperature stress alters the expression of phytoene desaturase genes (*crtP1* and *crtP2*) and the ζ-carotene desaturase gene (*crtQ*) together with the cellular carotenoid content of *Euglena gracilis*. Plant Cell Physiol. 60, 274–284. https://doi.org/10.1093/pcp/pcy208.

Krasny, L., Bland, P., Kogata, N., Wai, P., Howard, B.A., Natrajan, R.C., Huang, P.H., 2018. SWATH mass spectrometry as a tool for quantitative profiling of the matrisome. J Proteomics 189, 11–22. https://doi.org/10.1016/j.jprot.2018.02.026.

León-Vaz, A., León, R., Díaz-Santos, E., Vigara, J., Raposo, S., 2019. Using agro-industrial wastes for mixotrophic growth and lipids production by the green microalga *Chlorella sorokiniana*. N. Biotech. 51, 31–38. https://doi.org/10.1016/j.nbt.2019.02.001.

Li, H., Nguyen, H., Loo, R., Campuzano, I., Loo, J., 2018. An integrated native mass spectrometry and top-down proteomics method that connects sequence to structure and function of macromolecular complexes. Nat. Chem. 10, 139–148. https://doi.org/10.1038/nchem.2908.

Li, H., Watson, J., Zhang, Y., Lu, H., Liu, Z., 2020. Environment-enhancing process for algal wastewater treatment, heavy metal control and hydrothermal biofuel production: a critical review. Bioresour. Technol. 298, 122421. https://doi.org/10.1016/j.biortech.2019.122421.

Lin, Q., Liang, J.-R., Huang, Q.-Q., Luo, C.-S., Anderson, D.M., Bowler, C., Chen, C.-P., Li, X.-S., Gao, Y.-H., 2017. Differential cellular responses associated with oxidative stress and cell fate decision under nitrate and phosphate limitations in *Thalassiosira pseudonana*: comparative proteomics. PloS One 12, e0184849. https://doi.org/10.1371/journal.pone.0184849.

Ma, H., Zou, D., Wen, J., Ji, Z., Gong, J., Liu, C., 2018. The impact of elevated atmospheric CO_2 on cadmium toxicity in *Pyropiahaitanensis* (Rhodophyta). Environ. Sci. Pollut. Res. 25, 33361–33369. https://doi.org/10.1007/s11356-018-3289-z.

Marchello, A.E., Oliveira, N.L., Lombardi, A.T., Polpo, A., 2018. An investigation onto Cd toxicity to freshwater microalga *Chlorella sorokiniana* in mixotrophy and photoautotrophy: a Bayesian approach. Chemosphere 211, 794–803. https://doi.org/10.1016/j.chemosphere.2018.08.019.

Mi, H., Huang, X., Muruganujan, A., Tang, H., Mills, C., Kang, D., Thomas, P.D., 2017. PANTHER version 11: expanded annotation data from Gene Ontology and Reactome pathways, and data analysis tool enhancements. Nucleic Acids Res. 45, D183–d189. https://doi.org/10.1093/nar/gkw1138.

Miflin, B.J., Habash, D.Z., 2002. The role of glutamine synthetase and glutamate dehydrogenase in nitrogen assimilation and possibilities for improvement in the nitrogen utilization of crops. J. Exp. Bot. 53 (370), 979–987. https://doi.org/10.1093/jexbot/53.370.979.

Morelli, E., Scarano, G., 2004. Copper-induced changes of non-protein thiols and antioxidant enzymes in the marine microalga *Phaeodactylum tricornutum*. Plant Sci. 167, 289–296. https://doi.org/10.1016/j.plantsci.2004.04.001.

Mu, C., Zhang, S., Yu, G., Chen, N., Li, X., Liu, H., 2013. Overexpression of small heat shock protein LimHSP16.45 in *Arabidopsis* enhances the tolerance to abiotic stress. PloS One 8, e82264. https://doi.org/10.1371/journal.pone.0082264.g001.

Newton, R.J., McClary, J.S., 2019. The flux and impact of wastewater infrastructure microorganisms on human and ecosystem health. Curr. Opin. Biotechnol. 57, 145–150. https://doi.org/10.1016/j.copbio.2019.03.015.

Olguín, E.J., Sánchez-Galván, G., 2012. Heavy metal removal in phytofiltration and phycoremediation: the need to differentiate between bioadsorption and bioaccumulation. N. Biotech. 30, 3–8. https://doi.org/10.1016/j.nbt.2012.05.020.

Poirier, I., Pallud, M., Kuhn, L., Hammann, P., Demortière, A., Jamali, A., Chicher, J., Caplat, C., Gallon, R.K., Bertrand, M., 2018. Toxicological effects of CdSe nanocrystals on the marine diatom *Phaeodactylum tricornutum*: the first mass spectrometry-based proteomic approach. Ecotoxicol. Environ. Saf. 152, 78–90. https://doi.org/10.1016/j.ecoenv.2018.01.043.

Pundir, S., Martin, M.J., O'Donovan, C., UniProt, C., 2016. UniProt tools. Curr Protoc Bioinformatics 53, 1 29 21–15. https://doi.org/10.1002/0471250953.bi0129s53.

Rengel, R., Smith, R.T., Haslam, R.P., Sayanova, O., Vila, M., León, R., 2018. Overexpression of acetyl-CoA synthetase (*ACS*) enhances the biosynthesis of neutral lipids and starch in the green microalga *Chlamydomonas reinhardtii*. Algal Res 31, 183–193. https://doi.org/10.1016/j.algal.2018.02.009.

Rihab, B.A., Sabrine, B.O., Lina, C., Imed, M., Hatem, B.O., Ali, O., 2016. Cadmium effect on physiological responses of the tolerant Chlorophyta specie *Picocystis sp.* isolated from Tunisian wastewaters. Environ. Sci. Pollut. Res. 24, 1803–1810. https://doi.org/10.1007/s11356-016-7950-0.

Sewelam, N., Kazan, K., Hüdig, M., Maurino, V.G., Schenk, P.M., 2019. The AtHSP17.4C1 gene expression is mediated by diverse signals that link biotic and abiotic stress factors with ROS and can be a useful molecular marker for oxidative stress. Int. J. Mol. Sci. 20, 3201. https://doi.org/10.3390/ijms20133201.

Shanker, A., Cervantes, C., Lozatavera, H., Avudainayagam, S., 2005. Chromium toxicity in plants. Environ. Int. 31, 739–753. https://doi.org/10.1016/j.envint.2005.02.003.

Singh, S., Parihar, P., Singh, R., Singh, V.P., Prasad, S.M., 2016. Heavy metal tolerance in plants: role of transcriptomics, proteomics, metabolomics, and ionomics. Front. Plant Sci. 6 https://doi.org/10.3389/fpls.2015.01143.

Szklarczyk, D., Franceschini, A., Wyder, S., Forslund, K., Heller, D., Huerta-Cepas, J., Simonovic, M., Roth, A., Santos, A., Tsafou, K.P., Kuhn, M., Bork, P., Jensen, L.J.,

von Mering, C., 2015. STRING v10: protein–protein interaction networks, integrated over the tree of life. Nucleic Acids Res. 43, D447–D452. https://doi.org/10.1093/nar/gku1003.

Thangaraj, S., Shang, X., Sun, J., Liu, H., 2019. Quantitative proteomic analysis reveals novel insights into intracellular silicate stress-responsive mechanisms in the diatom *Skeletonema dohrnii*. Int. J. Mol. Sci. 20, 2540. https://doi.org/10.3390/ijms20102540.

Tchounwou, P.B., Yedjou, C.G., Patlolla, A.K., Sutton, D.J., 2012. Heavy metals toxicity and the environment. EXS 101, 133–164. https://doi.org/10.1007/978-3-7643-8340-4_6.

Varela, J.C., Pereira, H., Vila, M., León, R., 2015. Production of carotenoids by microalgae: achievements and challenges. Photosynth. Res. 125, 423–436. https://doi.org/10.1007/s11120-015-0149-2.

Vega, J.M., Garbayo, I., Domínguez, M.J., Vigara, J., 2006. Effect of abiotic stress on photosynthesis and respiration in *Chlamydomonas reinhardtii*. Enzym. Microb. Technol. 40, 163–167. https://doi.org/10.1016/j.enzmictec.2005.10.050.

Vega, J.M., 2019. Nitrogen and Sulfur Metabolism in Microalgae and Plants: 50 Years of Research Progess in Botany 81. Springer 1st Edition, pp. 1–40. https://doi.org/10.1007/978-3-030-36327-7.

Vizcaino, J.A., Csordas, A., del-Toro, N., Dianes, J.A., Griss, J., Lavidas, I., Mayer, G., Perez-Riverol, Y., Reisinger, F., Ternent, T., Xu, Q.W., Wang, R., Hermjakob, H., 2016. 2016 update of the PRIDE database and its related tools. Nucleic Acids Res. 44, D447–D456. https://doi.org/10.1093/nar/gkv1145.

Vowinckel, J., Capuano, F., Campbell, K., Deery, M.J., Lilley, K.S., Ralser, M., 2013. The beauty of being (label)-free: sample preparation methods for SWATH-MS and next-generation targeted proteomics. F1000Res 2, 272. https://doi.org/10.12688/f1000research.2-272.v2.

Wase, N., Black, P.N., Stanley, B.A., DiRusso, C.C., 2014. Integrated quantitative analysis of nitrogen stress response in *Chlamydomona sreinhardtii* using metabolite and protein profiling. J. Proteome Res. 13, 1373–1396. https://doi.org/10.1021/pr400952z.

Ye, M., Li, G., Yan, P., Ren, J., Zheng, L., Han, D., Sun, S., Huang, S., Zhong, Y., 2017. Removal of metals from lead-zinc mine tailings using bioleaching and followed by sulfide precipitation. Chemosphere 185, 1189–1196. https://doi.org/10.1016/j.chemosphere.2017.07.124.

Yoshida, N., Ikeda, R., Okuno, T., 2006. Identification and characterization of heavy metal-resistant unicellular alga isolated from soil and its potential for phytoremediation. Bioresour. Technol. 97, 1843–1849. https://doi.org/10.1016/j.biortech.2005.08.021.

Zhang, L., Lyu, K., Wang, N., Gu, L., Sun, Y., Zhu, X., Wang, J., Huang, Y., Yang, Z., 2018. Transcriptomic analysis reveals the pathways associated with resisting and degrading microcystin in *Ochromonas*. Environ. Sci. Technol. 52, 11102–11113. https://doi.org/10.1021/acs.est.8b03106.

Zhou, Q., Yang, Y., Yang, Z., 2019. Molecular dissection of cadmium-responsive transcriptome profile in a low-cadmium-accumulating cultivar of *Brassica parachinensis*. Ecotoxicol. Environ. Saf. 176, 85–94. https://doi.org/10.1016/j.ecoenv.2019.03.077.

Zhou, X., He, L., Wu, C., Zhang, Y., Wu, X., Yin, Y., 2017. Serine alleviates oxidative stress via supporting glutathione synthesis and methionine cycle in mice. Mol. Nutr. Food Res. 61, 1700262. https://doi.org/10.1002/mnfr.201700262.

Zhu, H., Ai, H., Cao, L., Sui, R., Ye, H., Du, D., Sun, J., Yao, J., Chen, K., Chen, L., 2018. Transcriptome analysis providing novel insights for Cd-resistant tall fescue responses to Cd stress. Ecotoxicol. Environ. Saf. 160, 349–356. https://doi.org/10.1016/j.ecoenv.2018.05.066.

Zhu, Q.-L., Guo, S.-N., Wen, F., Zhang, X.-L., Wang, C.-C., Si, L.-F., Zheng, J.-L., Liu, J., 2019. Transcriptional and physiological responses of *Dunaliella salina* to cadmium reveals time-dependent turnover of ribosome, photosystem, and ROS-scavenging pathways. Aquat. Toxicol. 207, 153–162. https://doi.org/10.1016/j.aquatox.2018.12.007.